



Published in final edited form as:

Org Lett. 2013 February 15; 15(4): 780–783. doi:10.1021/ol303435y.

Genome Mining of a Prenylated and Immunosuppressive Polyketide from Pathogenic Fungi

Yit-Heng Chooi[†], Jinxu Fang[§], Hong Liu^{||}, Scott G. Filler^{⊥,||}, Pin Wang[§], and Yi Tang^{*,†,‡}

Department of Chemical and Biomolecular Engineering, and Department of Chemistry and Biochemistry, University of California, Los Angeles, CA 90066, United States; Department of Chemical Engineering and Materials Science, University of Southern California, Los Angeles, CA 90089, United States; Los Angeles Biomedical Research Institute at Harbor-UCLA Medical Center, Torrance, CA 90502, United States; David Geffen School of Medicine at UCLA, Los Angeles, CA 90095, United States

Abstract



Activation of the polycyclic polyketide prenyltransferases (pcPTase)-containing silent clusters in *Aspergillus fumigatus* and *Neosartorya fischeri* led to isolation of a new metabolite neosartoricin (3). The structure of 3 was solved by X-ray crystallography and NMR to be a prenylated anthracenone. 3 Exhibits T-cell antiproliferative activity with an IC_{50} of 3 μ M, suggestive of a physiological role as an immunosuppressive agent.

Genome mining of sequenced microorganisms has yielded new natural products with interesting activities.¹ Mining of pathogenic species may yield new virulence factors or compounds active against human targets that are not produced in routine laboratory culturing conditions. As part of our efforts to understand fungal polyketide biosynthesis, we recently identified a group of polycyclic prenyltransferases (pcPTases) that catalyze the Friedel-Crafts transfer of C5 and C10 prenyl groups to aromatic polyketides. Phylogenetic

yitang@ucla.edu.

[†]Department of Chemical and Biomolecular Engineering, UCLA.

[‡]Department of Chemistry and Biochemistry, UCLA.

[§]University of Southern California, Los Angeles.

[⊥]David Geffen School of Medicine, UCLA.

^{||}Los Angeles Biomedical Research Institute.

Supporting Information Available NMR and MS characterization of compounds and additional experimental information and discussion. CIF Crystallographic Information File of compound 3 (CCDC 866028).

analyses showed that the homologous pcPTase genes formed a distinct clade from the common indole prenyltransferase.² The pcPTases are found mostly in the aspergillosis- and keratitis-causing *Aspergillus fumigatus* and *Neosartorya fischeri*, and the seven genome-sequenced arthrodermataceous dermatophytes.³

Interestingly, all these pcPTase genes are associated with a three-gene ensemble that makes polycyclic aromatic polyketides such as anthracenones (e.g. asperthecin) and naphthacenediones (e.g. TAN-1612 **1**, viridicatumtoxin).^{4,5} The ensemble includes genes that encode a non-reducing polyketide synthase (NR-PKS), a flavin-dependent monooxygenase (FMO) and a metallo- β -lactamase-like thioesterase (M β L-TE) (Figure 1). The prevalence of these pcPTase-encoding gene clusters among human and animal-associated fungi has invited the speculation that they may encode for production of a group of structurally-related prenylated polycyclic polyketides that have a common ecological role. When cloned and assayed in vitro, pcPTases from *N. fischeri*, *M. canis* and *T. tonsurans* were confirmed to be dimethylallyltransferases that can utilize naphthacenedione substrates including **1** (Scheme 1), supporting the hypothesis that prenylated polycyclic compounds may be produced by these organisms.

Using the *N. fischeri* pcPTase (NFIA_112230, Nf-NscD) as a lead, we aim to identify the compound(s) produced by the gene cluster (designated as *nsc* gene cluster). We expect the highly homologous and syntenic *nsc* cluster (Afu7g00120-170) in *A. fumigatus* to encode for identical metabolite(s) as in *N. fischeri* (>90% protein identities, Table S2). Under our laboratory culturing conditions, neither *N. fischeri* NRRL 181 nor *A. fumigatus* Af293 produced any detectable prenylated polyaromatics, consistent with the lack of such compounds associated with strains in literature.

Reverse transcriptase-PCR (RT-PCR) from the total RNA of *N. fischeri* did not detect transcription of the *nsc* cluster genes (Figure S1A), suggesting that the cluster is transcriptionally silent. To activate the pathway, we overexpressed a putative pathway-specific Zn(II)₂Cys₆ transcriptional factor (FTF) encoded by NFIA_112260 (Nf-*nscR*), a strategy that has been successfully used in various fungi recently.^{4,6} Transformation of *N. fischeri* with pBGP-Nf112260, which places *nscR* under the regulation of *A. nidulans* *gpdA* promoter (*P_{gpdA}*) and contains the *bar* resistance gene, resulted in several glufosinate-resistant colonies that exhibit yellow pigmentation on the reverse side on agar plates (Figure S1B). Diagnostic PCR confirmed the integration of *nscR*-overexpression cassette in transformant T2, while RT-PCR analysis showed that the *nsc* genes (*nscA-E*) were indeed upregulated (Figure S1A).

The transformant T2 cultured in stationary liquid GMM culture was extracted after 3 days. LC/MS analysis of the extract indicates production of multiple new compounds that are not found in the wild type *N. fischeri* (Figure 2A). All the new compounds exhibit similar UV spectra and λ_{max} between 395–410 nm, while the MW range from 358 to 484. We reasoned that the higher MW peaks, including **3** (m/z 485 [M+H]⁺) and **7** (m/z 425 [M+H]⁺) at later RT are likely to be prenylated, while the compounds at earlier RT are unprenylated intermediates and shunt products, i.e. **4** (m/z = 359 [M+H]⁺) and **8** (m/z = 317 [M+H]⁺) (Figure 2A and Figure S2). To investigate if the same set of metabolites is produced by *A.*

fumigatus upon transcriptional activation of the syntenic *nsc* cluster (Figure 1), an overexpression cassette encoding the putative FTF Afu7G00170 (p402-Af0170) with the resistance marker *phleo^R* for selection was randomly integrated into the genome. In identical fashion to *N. fisheri*, *A. fumigatus* incorporating the cassette exhibits yellow pigmentation. The metabolite profile of *A. fumigatus* T1 is indeed identical to *N. fisheri* T2 based on UV spectra, retention time and *m/z* values of major compounds **3**, **4**, **7** and **8** during LC-MS analysis (Figure S3). Thus, both clusters in *N. fisheri* and *A. fumigatus* have been activated to produce the same set of new metabolites.

About 35 mg of **3** (as bright yellow, amorphous powder) was successfully purified from 2 L of the *N. fisheri* T2 culture. Orange platelet-like crystals were obtained in an EtOAc/*n*-hexane solvent system and the atom connectivity of **3** was resolved by X-ray diffraction (Figure 2B). **3** Apparently co-crystallized with residual DMSO-*d*₆ from NMR analyses. Anomalous scattering of the X-rays by the sulfur atom in DMSO allowed elucidation of the absolute three-dimensional structure of **3**. The X-ray structure assisted in the assignment of the NMR spectra (Table S2). The structure of **3** consists of a tricyclic 3,4-dihydroanthracen-1(2*H*)-one core with a 2,4-keto-enol pentyl side chain extending from a decaketide (C₂₀) backbone, a dimethylallyl side chain at C5, and a C2-acetoxy substitution *syn* to a C3-hydroxyl. The 2,4-keto-enol pentyl chain tautomerizes in organic solvent, where the β -keto-enol form is dominant over the β -diketo form as observed in the ¹H, ¹³C and 2D NMR spectra (Table S2 and Figure S5–S8). **3** was named neosartoricin, based on the common distribution in both *N. fisheri* and *A. fumigatus* (given the Teleomorph name *Neosartorya fumigata*).⁷ Besides **3**, the desacetyl derivative **7** (overlapped with **3** in Figure 2A) was isolated in small quantity from the *N. fisheri* T2. Due to low titer (<1 mg/L) and instability upon purification, only ¹H-NMR and LCMS data can be obtained for **7**. Spectra analysis and comparison to **3** led to assignment of the structure in Scheme 2 (Table S3). **4** and **8** are non-prenylated anthracenones derived from a decaketide and a nonaketide (C₁₈) respectively. Both compounds were isolated and characterized from yeast expressing the NR-PKS and FMO pair from the *A. niger ada* pathway for **1** and *A. nidulans apt* pathway for asperthecin, previously.⁴

A pathway for biosynthesis of **3** was proposed based on analysis of the intermediates (Scheme 2 and Figure S2). As NscA-C are highly homologous to AdaA-C in *A. niger*, the biosynthesis of the anthracenones portion of **3** is likely to follow a parallel pathway for that of **1**: NscA synthesizes and cyclizes the decaketide backbone; NscB mediates the product release through hydrolysis followed by spontaneous decarboxylation to afford **4**; and NscC is responsible for the stereospecific hydroxylation at C2. The NscD catalyzes the addition of dimethylallyl group to the aromatic C5, consistent with the previously determined regioselectivity (Scheme 1). The timing of NscC, which was proposed to occur after prenylation of **4** to yield **5**, likely directs the formation of the anthracenone present in **6** instead of the naphthacenedione in **1**, although an alternative pathway via a Baeyer-Villiger cleavage of the fourth ring, such as that observed in mithramycin pathway,⁸ cannot be completely ruled out (See Supplementary Discussion). There is no gene encoding *O*-acetyltransferase in the *nsc* gene cluster; thus, the 2-*O*-acetylation of **6** to **3** maybe catalyzed

by an unidentified *O*-acetyltransferase in *N. fisheri*, while off-pathway dehydration of **6** affords **7**.

3 Does not exhibit significant inhibitory activity against either Gram positive or Gram negative bacteria, nor the yeasts *Saccharomyces cerevisiae* and *Candida albicans* (> 64 µg/mL). We tested **3** for immunosuppressive activity in a cell-based in vitro assay, which showed that **3** exhibits antiproliferative activity on anti-CD3/CD28-activated murine splenic T-cells with an IC₅₀ of 2.99 µM (1.45 Vg/mL) (Figure 3A). The effect of **3** on [³H]-thymidine uptake by murine T-cells is dosage-dependent. Cyclosporin A (CsA) was used as a control in the assay and was shown to exhibit an IC₅₀ of 26 nM, which is comparable to the value reported previously.⁹ Next, we included compound **1**, **2**, **4**, **7**, and **8** in a structural-activity relationship studies along with emodin, which has been previously shown to exhibit moderate immunosuppressive activity.¹⁰ The data show that **3** exhibits a higher inhibitory activity compared to all the analogs tested including emodin (Figure 3B) and that the dimethylallyl group and *O*-acetyl is required for its activity. **3** Was then assayed for cytotoxicity against HeLa and HFF cells, which shows that **3** is less toxic to the two cell lines compared to **1** and **2** at up to 50 µM concentration, suggesting that the antiproliferative activity of **3** is relatively specific to T-cells (Figure S9).

We next examined the possible role of **3** in establishing primary infection in human hosts with a ⁵¹Cr release cell damage assay on A549 lung epithelial cells and RAW 264.7 macrophage cells. **3** Does not appear to cause any damage to both cell types up to 10 µM (< 5% specific release). The extent of A549 cell damage caused by the *nsc* pathway-overexpressing *A. fumigatus* T1 in vitro was also investigated, but no statistically significant differences in cell damage was observed compared to wild type *A. fumigatus* (Figure S10). Thus, we concluded that the *nsc* pathway compounds including **3** are not involved in primary virulence but may facilitate infection through suppressing the host adaptive immunity.¹¹

Supplementary Material

Refer to Web version on PubMed Central for supplementary material.

Acknowledgments

We thank Dr. Saeed Khan at the UCLA crystallography facility for solving the X-ray structures. Anu Biswas and Muxun Zhao of UCLA are thanked for their assistance in cytotoxicity assays. This work is supported by NIH 1R01GM085128 and 1DP1GM106413 to YT, and R01AI073829 to SGF.

References

1. Winter JM, Behnken S, Hertweck C. *Curr Opin Chem Biol.* 2011; 15:22. [PubMed: 21111667]
2. Chooi YH, Wang P, Fang J, Li Y, Wu K, Tang Y. *J Am Chem Soc.* 2012; 134:9428. [PubMed: 22590971]
3. Martinez DA, Oliver BG, Graser Y, Goldberg JM, Li W, Martinez-Rossi NM, Monod M, Shelest E, Barton RC, Birch E, Brakhage AA, Chen Z, Gurr SJ, Heiman D, Heitman J, Kosti I, Rossi A, Saif S, Samalova M, Saunders CW, Shea T, Summerbell RC, Xu J, Young S, Zeng Q, Birren BW, Cuomo CA, White TC. *MBio.* 2012; 3:e00259. [PubMed: 22951933]

4. Li Y, Chooi Y-H, Sheng Y, Valentine JS, Tang Y. *J Am Chem Soc.* 2011; 133:15773. [PubMed: 21866960]
5. Chooi YH, Cacho R, Tang Y. *Chem Biol.* 2010; 17:483. [PubMed: 20534346]
6. Bergmann S, Schumann J, Scherlach K, Lange C, Brakhage AA, Hertweck C. *Nat Chem Biol.* 2007; 3:213. [PubMed: 17369821]
7. O’Gorman CM, Fuller HT, Dyer PS. *Nature.* 2008; 457:471. [PubMed: 19043401]
8. Gibson M, Nur-e-alam Mohammad, Lipata F, Oliveira MA, Rohr J. *J Am Chem Soc.* 2005; 127:17594. [PubMed: 16351075]
9. Zenke G, Strittmatter U, Fuchs S, Quesniaux VFJ, Brinkmann V, Schuler W, Zurini M, Enz A, Billich A, Sanglier JJ. *J Immunol.* 2001; 166:7165. [PubMed: 11390463]
10. Huang HC, Chu SH, Chao PDL. *Eur J Pharmacol.* 1991; 198:211. [PubMed: 1830846]
11. Blanco JL, Garcia ME. *Vet Immunol Immunopathol.* 2008; 125:47. [PubMed: 18565595]

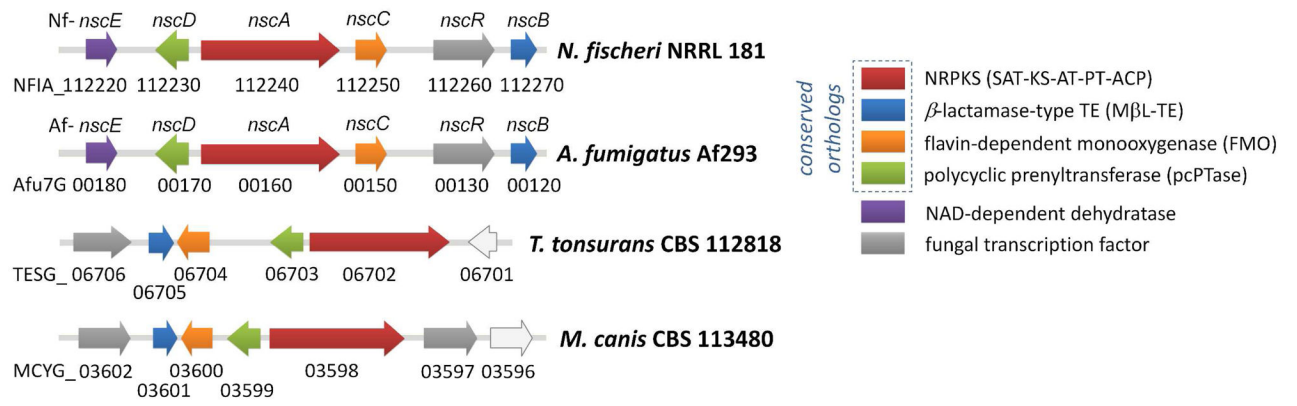


Figure 1. Evolutionary conserved pcPTase-containing gene clusters in *N. fischeri*, *A. fumigatus*, *T. tonsurans* and *M. canis*.

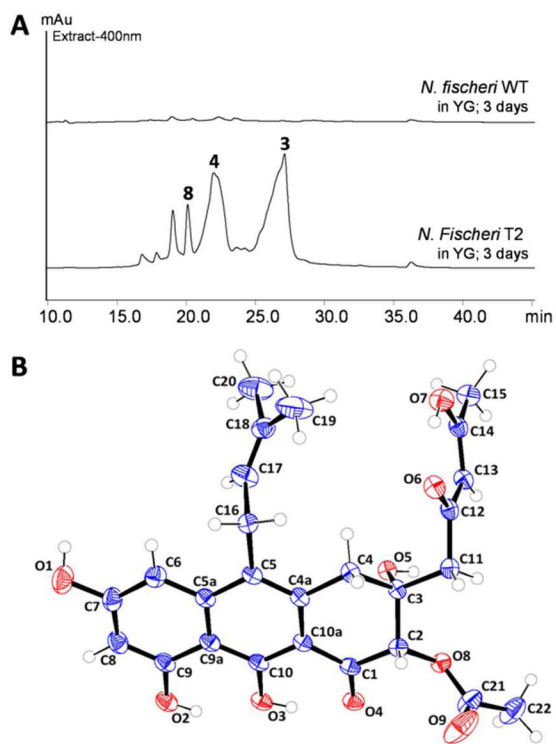


Figure 2. Activation of a silent pathway in *N. fischeri*. (A) Metabolic profile of *N. fischeri* T2 (*nscR* overexpression) compared to WT. (B) Perspective drawing of the molecular confirmation of neosartoricin 3.

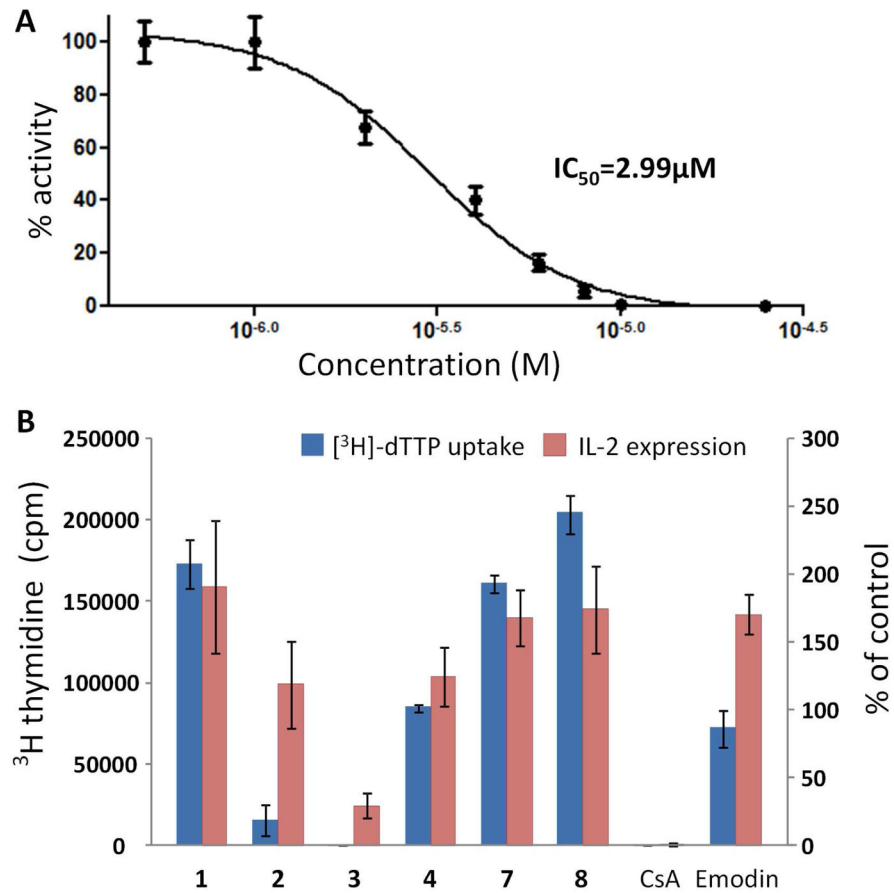
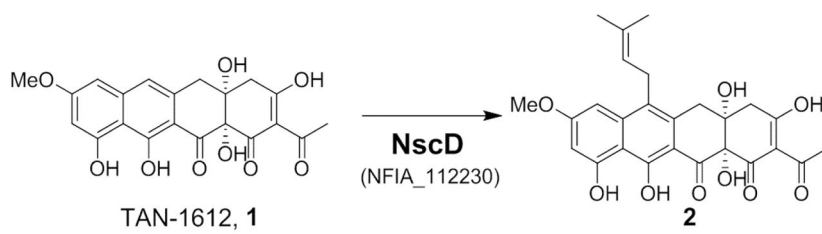
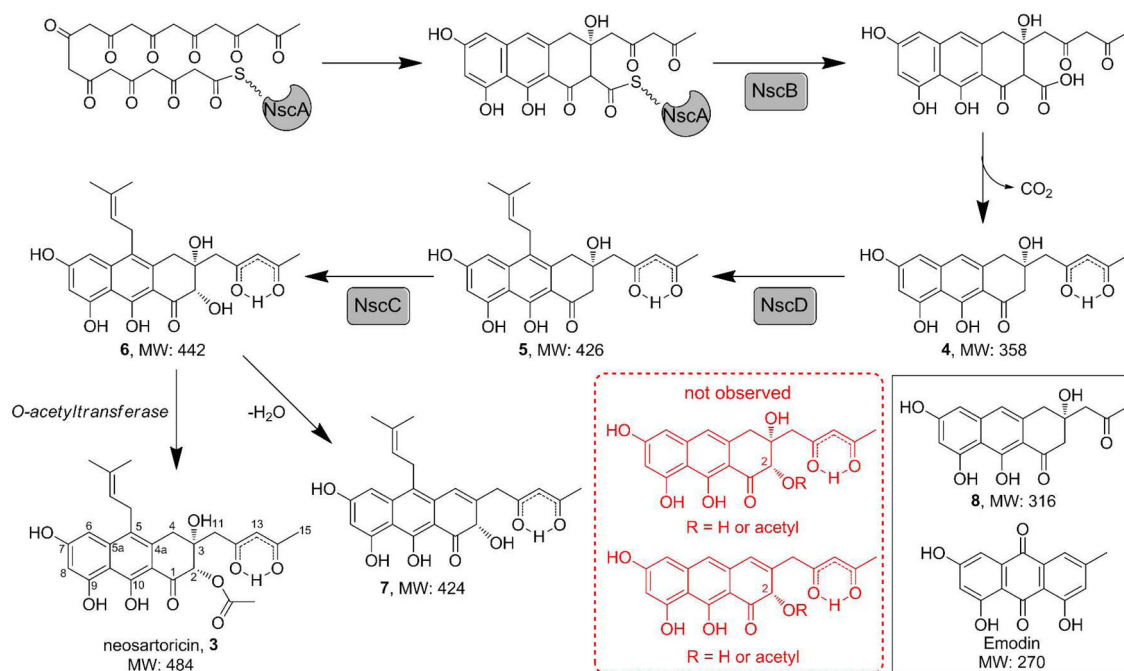


Figure 3. Effect of **3** on murine T-cell proliferation. (A) Dose-response curve of **3** on [³H]-thymidine uptake by murine T-cells (% of DMSO control). (B) Comparison of the activity of **3** with **1**, **2**, **4**, **7**, **8**, cyclosporine A (CsA) and emodin at 10 μM concentration.



Scheme 1.
Conversion of **1** to **2** by pcPTase NscD.

**Scheme 2.**Proposed pathway for biosynthesis of **3**

See Figure S2 and Supplementary Discussion for more details.